LETTER Communicated by Misha Tsodyks

Spike-Driven Synaptic Dynamics Generating Working Memory States

Daniel J. Amit
daniel.amit@roma1.infn.it
Gianluigi Mongillo
mongillo@titanus.roma1.infn.it
Dipartimento di Fisica, Universita' di Roma, La Sapienza, 00185 Rome, Italy, and Racah Institute of Physics, Hebrew University, Jerusalem, Israel

The collective behavior of a network, modeling a cortical module of spiking neurons connected by plastic synapses is studied. A detailed spike-driven synaptic dynamics is simulated in a large network of spiking neurons, implementing the full double dynamics of neurons and synapses. The repeated presentation of a set of external stimuli is shown to structure the network to the point of sustaining working memory (selective delay activity). When the synaptic dynamics is analyzed as a function of pre- and postsynaptic spike rates in functionally defined populations, it reveals a novel variation of the Hebbian plasticity paradigm: in any functional set of synapses between pairs of neurons (e.g., stimulated–stimulated, stimulated–delay, stimulated–spontaneous), there is a finite probability of potentiation as well as of depression. This leads to a saturation of potentiation or depression at the level of the ratio of the two probabilities. When one of the two probabilities is very high relative to the other, the familiar Hebbian mechanism is recovered. But where correlated working memory is formed, it prevents overlearning. Constraints relevant to the stability of the acquired synaptic structure and the regimes of global activity allowing for structuring are expressed in terms of the parameters describing the single-synapse dynamics. The synaptic dynamics is discussed in the light of experiments observing precise spike timing effects and related issues of biological plausibility.

1 Introduction

Long-term modifications of the synaptic efficacies are believed to affect information processing in the brain. The occurrence of such modifications would be manifest as the appearance of new patterns of neural activity. In both IT and PF cortex of monkeys, trained to perform a delayed-match-to-sample (DMS) task, small neural assemblies have been found to exhibit selective, persistent enhanced spike rates during the delay interval between successive stimulations (Miyashita, 1988; Miller, Erickson, & Des-

imone, 1996). This kind of activity is related to the ability of the monkey to hold an item in memory (Amit, 1995); indeed, it reflects the last stimulus seen. It will be referred to as working memory (WM) activity. WM appears only after a substantial training stage, during which, presumably, the local synaptic structure is modified by the incoming stimuli.[1] Then new patterns of neural activity appear.

Spiking neural network models indicate that the phenomenology observed in DMS tasks can be reproduced by coherent modifications of the synaptic efficacies (Amit & Brunel, 1997a; Amit, 1998). Specifically, the mean excitatory synaptic efficacy among neurons belonging to the selective population must increase, while the efficacies in synaptic population connecting selective to other neurons must decrease. Hence, one expects that the neural activity evoked by presentation of stimuli during the learning stage produces such modifications so that WM can appear. This raises the question of how the synaptic dynamics is related to the neural activity.

A simulation like the one presented here has multiple utility. First, it calls into focus certain features of the single synapse that should be clarified in biological investigation. Second, it provides a more complete benchmark (relative to simulations with fixed synapses), in the bridge between experiment and theory (Amit, 1998). And once the simulation clarifies the essential features of the microscopic synaptic dynamics, simplified (and hence faster) learning algorithms can be identified, to be used in simulating complex behavioral situations.

We first review the experimental protocols used to induce long-term synaptic modifications. Then we recapitulate a general model of spike-driven synaptic plasticity, proposed by Fusi, Annunziato, Badoni, Salamon, and Amit (2000) and discuss the extent to which this dynamics satisfies general desiderata and concords with experimental findings. The plastic synapse is then embedded in a full-scale simulation of a large network of spiking neurons. The synaptic dynamics is propelled purely by the actual spikes emitted by the neurons, as a consequence of a preassigned protocol of stimulus presentation, mimicking those used in the DMS tasks. It is shown that WM is actually formed in the process and that its slow formation can be qualitatively understood.

2 Experimental Protocols for LTP and LTD

Long-term potentiation (LTP) and long-term depression (LTD) are persistent changes in synaptic efficacy that are expected to be induced by patterns of pre- and postsynaptic activity. Hebbian tradition had these changes re-

[1] There are zones in cortex where the synaptic structure giving rise to delay activity may be built in (Kritzer & Goldman-Rakic, 1995; Compte, Brunel, Goldman-Rakic, & Wang, 2000). Those are outside the scope of our discussion.

lated to pre- and postsynaptic spike rates. A bridge between spikes and plasticity has been recently confirmed by detailed experimental studies. Specific, well-controlled stimulation protocols have been developed that reliably induce LTP and LTD in hippocampal and cortical synapses. However, certain questions remain open. Most important, we consider the passage from spike-induced synaptic plasticity to rate-dependent plasticity, so essential for the learning of working memory. The difficulty in providing such a bridge, from spikes to rates, opens up questions concerning the dependence of the effects observed on the specific details of the protocols used (see section 7.1). This calls for a closer identification of the neural activity parameters that control the synaptic transitions and determine the type of modification that occurs: LTP or LTD.

Some protocols for the induction of LTP and LTD involve repetitive presynaptic stimulation by electrical pulses (Dudek & Bear, 1992). The induction consists of a fixed number of several hundred (e.g., 600–900) pulses delivered at various frequencies. No experimental control is exercised on the postsynaptic activity, which is determined by the presynaptic activation. The experiments are carried out in slices from the CA1 region of the hippocampus, stimulating the Schaffer collateral afferents. Depending on the stimulation frequency, LTP or LTD is induced. The same protocols also induce reliably synaptic changes in the neocortex.

High-frequency stimulation is particularly effective in inducing LTP. On the other hand, presynaptic activation at low frequencies is likely to trigger homosynaptic LTD. More precisely, no plasticity is observed at frequencies less than 0.1 Hz, LTD is observed using 1 Hz stimulation, and LTP is observed using stimulation frequencies greater than 10 Hz (Bear, 1996).

This phenomenology is explained in the following way (Bear, 1996): Up- and down-regulation of synaptic strength depends on the postsynaptic intracellular concentration of calcium, which in turn depends on the level of postsynaptic membrane potential. If the level of $[Ca^{2+}]$ exceeds a threshold, the synapse tends to be potentiated. Otherwise, it tends to be depressed. High-frequency stimulation of a cell produces a higher level of postsynaptic depolarization, due to the fast temporal summation of excitatory postsynaptic potentials (EPSPs) and, hence, higher levels of $[Ca^{2+}]$. Stimulation at 10 Hz produces, on average, neither LTD nor LTP, which may indicate a critical level of postsynaptic $[Ca^{2+}]$ corresponding to the presynaptic activation. This hypothesis seems corroborated by other experiments (Steele & Mauk, 1999) in which the level of recurrent inhibition during the stimulation is pharmacologically controlled by using either agonist or antagonist of the GABA receptor. When antagonist is applied, the threshold frequency for LTP is decreased; if agonist is present, it is increased. When GABA antagonist is present, the recurrent inhibition is less effective. Accordingly, the depolarization level allowing for LTP can be reached with lower frequencies. The reasoning is analogous in the presence of the GABA agonist.

More recently, other stimulation protocols have been developed to induce long-term synaptic modifications in which postsynaptic activity also is experimentally controlled (Markram, Lübke, Frotscher, & Sakmann, 1997; Bi & Poo, 1998). In this experimental setup, both pre- and postsynaptic events are evoked by injecting current pulses into the cell body. Events are then coupled according to various protocols, varying either the temporal order between the pre- and postsynaptic events or the number and/or the frequency of pairing.

The role of the number of pre- and postsynaptic spike pairings is studied in Markram et al. (1997). A postsynaptic spike is evoked several milliseconds after presynaptic emission. Such pairing is repeated 2, 5, and 10 times, and the sequence is repeated 10 times every 4 seconds. The postsynaptic spikes are evoked at 20 Hz. In all these cases, LTP is observed. Subsequently, the frequency dependence has been studied according to the following protocol: five presynaptic spikes are paired, as previously described, with postsynaptic spikes at various frequencies. Again, the pairing is repeated 10 times every 4 seconds. It was found that no potentiation occurs if the frequency is lower than 10 Hz. For the dependence on the relative timing between pre- and postsynaptic spikes, it is found that LTP occurs if the presynaptic spike precedes the postsynaptic one, while if the presynaptic spike follows the postsynaptic one, the synapse undergoes LTD. It is also noted that if the temporal interval between the two events is too large, no synaptic modifications occur.

Bi and Poo (1998) determined the exact temporal window in which the occurrence of both pre- and postsynaptic emission is effective to induce long-term synaptic modifications. They coupled 60 presynaptic spikes delivered at 1 Hz with postsynaptic spikes by varying the temporal order of occurrence of the events (pre-post or post-pre) and the time difference between them. Synapses are strengthened if the presynaptic spikes precede postsynaptic spikes by less than 20 milliseconds and are weakened if instead presynaptic spikes follow postsynaptic spikes within the same interval.

Markram et al. (1997) did not find potentiation for presynaptic activation rates lower than 10 Hz, while Bi and Poo (1998) did find both potentiation and depression at 1 Hz. The seemingly inconsistent behavior could be due to the fact that while Markram et al.'s experiment was carried out with cortical cells, Bi and Poo worked with hippocampal synapses. An alternative explanation is based on the difference in the number of pairings in the two cases. In other words, 5 pairings at 1 Hz do not provoke LTP, whereas 60 at the same frequency increase the synaptic efficacy. This fact could be understood in the following way: Each pairing of pre- and postsynaptic spikes tends to modify the synaptic efficacy, but a single event does not trigger long-term modification. The effect of a single pairing should therefore decay with time, and it is the accumulation of the effects of several pairings that is required to trigger a long-lasting modification. To provoke LTP or LTD, a specific number of couplings must occur in a given time interval,

so the individual effects are not totally forgotten. The number of pairings with respect to the time interval could in principle be experimentally determined, furnishing information about the effect of a single pairing and its decay time.

Despite the somewhat contrasting conclusions reached using different protocols, as to the event that ultimately triggers the modifications, other properties of synaptic plasticity are widely accepted. Experiments in vitro and in vivo have shown that a synapse is bidirectionally modifiable (Dudek & Bear, 1993). In other words, the same synapse can undergo both LTP and LTD. Moreover, the same synapse once depressed can be newly potentiated by a suitable stimulation, and vice versa. However, the modification of the synaptic strength is prevented when NMDA receptors are blocked, regardless of the stimulation used (Dudek & Bear, 1992; Markram et al., 1997). An immediate action of the NMDA release is the opening of voltage-gated Ca^{2+} channels and the consequent influx of the calcium ions. When this is prevented, the expression of the synaptic plasticity is impaired; no transitions are observed. This fact seems to support the model in which intracellular calcium concentration is a fundamental parameter controlling LTP and LTD.

3 From Experiments to the Model

We now proceed to recapitulate the model of synaptic dynamics (Fusi et al., 2000) to be used as the learning element in the simulation. A plausible synaptic device would be able to maintain only a small number of discrete stable efficacies on long timescales. We choose the synapses to have two such states and to move between them stochastically. There is also some experimental evidence that synapses may in fact have only two stable values on a long timescale (Petersen, Malenka, Nicoll, & Hopfield, 1998) . In section 7.1, we show that our synapse is not inconsistent with the wealth of findings concerning synaptic plasticity at the individual synaptic level described in section 2. We have not opted for a detailed agreement with all these findings because quite a few of them are still rather tentative and because our objective has been to have a reasonable synapse for a first study of the formation of selective delay activity by the spikes produced in the course of the natural behavior of the neurons in a network.

3.1 A Model of Plastic Synapse. The plastic synapse is characterized by an internal analog variable X and a two-state value for its stable efficacy J_d, J_p (depressed and potentiated, respectively). The stable efficacy is in turn determined by X (Fusi et al., 2000; Del Giudice & Mattia, 2001). When X is above a threshold θ_X, the synapse is in its potentiated state of efficacy J_p. Otherwise, the synapse is in its depressed state $J_d (< J_p)$. A transition occurs when X crosses the synaptic threshold: if X crosses from below to above, the result is LTP ($J_d \rightarrow J_p$); if X crosses from above to below, the result is LTD ($J_p \rightarrow J_d$). X is restricted to the interval (0 and 1), whose end points are

reflecting barriers for the dynamics of X, and it obeys

$$\dot{X}(t) = R(t) + H(t), \tag{3.1}$$

where $R(t)$ is a refresh term, responsible for long-term state preservation. It drives X toward 0(1), depending on whether it is below (above) the synaptic threshold θ_X. This term mimics the biochemical mechanisms that keep synaptic efficacy stable in the absence of stimulation, against erasure by spontaneous activity. The dynamics of the drift we choose to be linear,

$$R(t) = -\alpha\Theta(-X + \theta_X) + \beta\Theta(X - \theta_X), \tag{3.2}$$

where $\Theta(\cdot)$ is the Heaviside function, $\Theta(x) = 1$ for $x > 0$ and 0 otherwise. This bistability is analogous to that of a computer DRAM memory bit. $H(t)$ relates the synaptic dynamics to the pre- and postsynaptic neural activities and is responsible for synaptic transitions. The synaptic efficacy is modifiable only when the synapse is activated by a presynaptic action potential. Hence, $H(t)$ should be different from zero only upon arrival of a presynaptic spike, which we express as

$$H(t) = \sum_k F(t_k^{pre})\delta(t - t_k^{pre}), \tag{3.3}$$

that is, a sum over all presynaptic spike emission times. A priori, the time of the synaptic activation does not coincide with the presynaptic emission. In fact, once an action potential is generated in the soma, it travels along the axon, reaching the synaptic boutons (synaptic activations). Here, the spike provokes the release of the neurotransmitter, which in turn provokes the current influx into the postsynaptic cell. The time elapsed from the presynaptic spike emission to the postsynaptic variation of the depolarization is the synaptic delay and is of the order of a couple of milliseconds. However, most of this time is associated with postsynaptic ionic flow along dendrites. The axonal delay is very short, and the synaptic activation coincides with the presynaptic emission.

Each spike induces a jump in X whose value is determined by $F(\cdot)$, which in turn depends on the state of the postsynaptic neuron at the time of the presynaptic emission. The complete specification of $H(t)$ requires the introduction of a neural model, which we assume to be that of an integrate-and-fire neuron (see section 4.1). One possibility is that F is determined by the intracellular concentration of calcium, as proposed by Bear (1996). $F(\cdot)$ would be positive when intracellular $[Ca^{2+}]$ exceeds some critical level and negative if it is below another critical level. We model this complex mechanism taking $F(\cdot)$ to be a function of the postsynaptic depolarization.[2] This

[2] This assumption seems to be corroborated by recent experimental evidences (Sjöström, Turrigiano, & Nelson, 2001). See also section 7.1.

may not be the final answer, but it can be judged by its performance for the special protocols used in experiments on plasticity and with respect to the distributed learning dynamics it generates in a network. The synaptic dynamics is then related to the neural dynamics by postulating

$$F(t^{pre}) = F(V_{post}(t^{pre})) = \begin{cases} a & \text{if } V_{post} > \theta_1 \\ -b & \text{if } V_{post} < \theta_2 \\ 0 & \text{otherwise,} \end{cases} \tag{3.4}$$

with $\theta_2 \leq \theta_1 < \theta$, where θ is the neural threshold for spike emission. V_{post} is the membrane depolarization of the postsynaptic neuron. Examples of synaptic dynamics for LTP and LTD are depicted in Figures 1 and 2, respectively.

3.2 Transition Probabilities. The temporal evolution of $H(t)$, and hence the dynamics of the synaptic internal variable $X(t)$, could in principle be determined by specifying the pre- and postsynaptic neural activity. The situation we are interested in is neurons embedded in a large recurrent network. In this case, neural firing is stochastic, principally due to the random pattern of connectivity (van Vreeswijk & Sompolinsky, 1996). As a consequence,

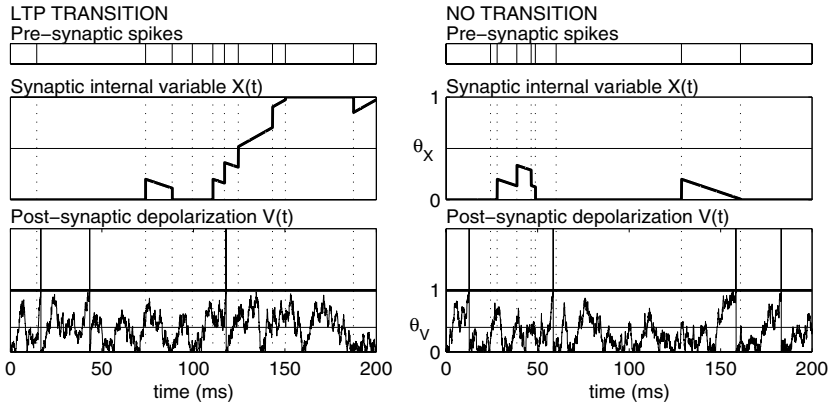

Figure 1: Synaptic dynamics. The time evolution of $X(t)$ (middle panel); following presynaptic emission (top), $X(t)$ is regulated up (down) if the postsynaptic depolarization $V(t)$ is greater (smaller) than $\theta_V (= \theta_1 \equiv \theta_2)$ (bottom). In the time intervals between spikes, $X(t)$ drifts linearly up or down, according to equation 3.2 (see text for details). (Left) LTP. The synapse starts from its depressed value J_d, (since $X < \theta_X$); by the end of the interval, it is potentiated to J_p, (since $X > \theta_X$). (Right) No transition. At the end of the interval, X returns to its initial value. The evolution of $V(t)$ is that of an integrate-and-fire neuron with a linear leakage current. For details see section 4.1. (Reproduced from Fusi et al., 2000.)

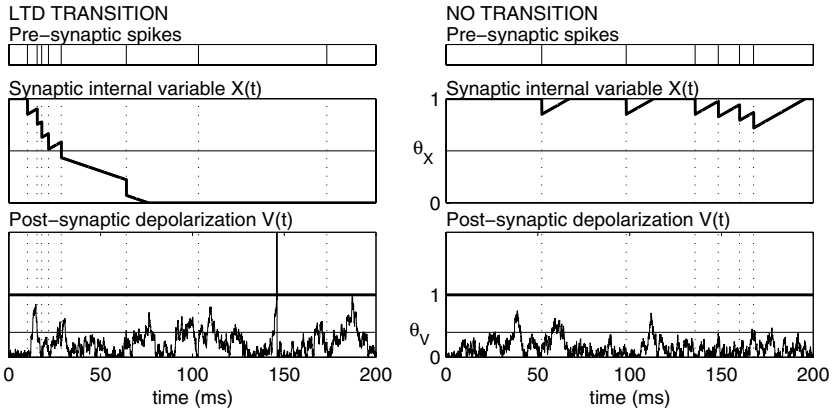

Figure 2: Synaptic dynamics. (Left) LTD. A presynaptic burst allows X to cross the threshold θ_X from above, provoking downregulation of synaptic efficacy ($J_p \to J_d$). (Right) No transition. Conventions as in Figure 1. (Reproduced from Fusi et al., 2000.)

long-term synaptic transitions are themselves stochastic, and it is possible to characterize them by a frequency-dependent transition probability. We define $P_{LTP}(\nu_{pre}, \nu_{post}, T)$ as the probability that a depressed synapse undergoes LTP during a time interval T of constant external afferents. ν_{pre} and ν_{post} are, respectively, the mean emission rates of the pre- and postsynaptic neuron. The probability of LTD, $P_{LTD}(\nu_{pre}, \nu_{post}, T)$, is defined analogously.

$P_{LTP}(\nu_{pre}, \nu_{post}, T)$ and $P_{LTD}(\nu_{pre}, \nu_{post}, T)$ contain the information relevant for the unsupervised learning dynamics. They can be estimated by simulating the coupled neural and synaptic dynamics as described in Fusi et al. (2000). Once they are known, it becomes possible to determine the regimes of network activity of plasticity (i.e., significant modifications of synaptic structure) and of overall structural stability (i.e., negligible modifications). It also becomes possible to estimate the number of synaptic transitions in a given synaptic population per stimulus presentation or, equivalently, the probability of transition per presentation. When these probabilities are known, the structuring process can be described in a compact form, obtaining the fraction of potentiated synapses in each population as a function of the number of stimulus presentations.

A simplified classification of the synaptic dynamics can be obtained in terms of $P_T \equiv P_{LTP} + P_{LTD}$ and $P_R \equiv P_{LTP}/P_T$ (see also Fusi et al., 2000). P_T is defined as the total transition probability, that is, the probability that a long-term transition occurs during T (either potentiation or depression), and P_R is defined as the relative probability of LTP with respect to LTD. When $P_R \sim 1$, LTP is likely to occur.

Suppose $a < \theta_X$ and $b < (1 - \theta_X)$, so that several jumps are required to cross synaptic threshold. When the presynaptic neuron fires, X is modified according to the value of the postsynaptic depolarization. If a further spike does not arrive to push X toward the threshold, the synaptic internal state is reset by the refresh current, to either 0 or 1, depending on whether X is above or below its threshold (see equation 3.2). The time to forget completely a given jump in X is the ratio between the amplitude of the jump and the synaptic refresh current. In the synaptic device described here, we have a reset time for potentiation $\tau_p (= a/\alpha)$ and one for depression $\tau_d (= b/\beta)$. To simplify the reasoning, we suppose $\tau_p = \tau_d$.

Transitions typically would be provoked by bursts of presynaptic spikes. A burst can cause a transition if the time intervals between successive spikes (ISI) are on average shorter than τ_p. In this case (the high presynaptic rate regime), a long-term synaptic transition, either up or down, can occur. When the mean ISI is greater than τ_p (the low presynaptic rate regime), the probability of a synaptic transition is negligible. Consequently, P_T is zero if $\nu_{pre} \ll 1/\tau_p$ and is an increasing function of the presynaptic emission rates for $\nu_{pre} > 1/\tau_p$.

The direction of a jump in the synaptic internal variable depends on the value of the postsynaptic depolarization (see equation 3.4). The relative frequency of upregulation of X ($X \to X + a$) with respect to that of downregulation ($X \to X - b$) increases with postsynaptic emission rates. Indeed, to emit at high rates, the postsynaptic depolarization must often be near the threshold and, hence, $V > \theta_1$. On the other hand, when the postsynaptic neuron is emitting at a low rate, its depolarization is fluctuating around the rest potential, and hence below θ_2, so P_R would be an increasing function of ν_{post}.

We have argued that the synaptic device behaves in a Hebbian way. In other words, a synapse between two neurons, both emitting at a high rate, tends to be potentiated ($P_T > 0$, $P_R \sim 1$), while a synapse connecting a high-rate presynaptic neuron to a low-rate postsynaptic one tends to be depressed ($P_T > 0$, $P_R \sim 0$). In fact, as we shall see, a dynamic synapse naturally extends the plasticity scenario: synapses in neural populations where one would expect LTP may undergo LTD, and vice versa. This may be due to fluctuations or to the width of the emission rate distribution in a functionally uniform neural population. When the average rates are high and close to each other in the pre- and postsynaptic cells or if there is a very large difference between the two, deviations are few, and Hebb is maintained to a very good accuracy. But if the average rates are closer, as would, for example, be the case when one population of neurons is stimulated and another is in enhanced delay activity (the substrate for the generation of context-correlations; Miyashita, 1988; Brunel, 1996), or of pair-associate representations (Sakay & Miyashita, 1991; Erickson & Desimone, 1999), LTP and LTD probabilities for the synapses connecting the two populations would both be significant. The one for LTP would be higher to allow the association.

The structuring in that population will not go on indefinitely (creating representation collapse), but will saturate at a level determined by the ratio of the two probabilities, a very welcome modification that will be explored in depth elsewhere (Mongillo & Amit, 2001a).

4 Simulations

4.1 Single Cell Model. As a model of the spiking neuron we use the linear integrate-and-fire (LIF) model of Fusi and Mattia (1999) because it has been found to be consistent with the behavior of real cells in noisy conditions (Rauch, La Camera, Lüscher, Senn, & Fusi, 2002) and also because of its analytical tractability. Despite its simplicity, this neural model is able to reproduce much of the phenomenology of networks of RC integrate-and-fire neurons (Fusi & Mattia, 1999; Mongillo & Amit, 2001b). It is characterized by a firing threshold θ, a (postspike) reset potential V_r, a constant leakage current β_I, and a refractory period τ_{arp}. The evolution of the membrane depolarization below threshold is

$$\dot{V} = \begin{cases} -\beta_I + I(t) & \text{if } V(t) > 0 \\ 0 & \text{if } V(t) = 0 \text{ and } \dot{V} < 0. \end{cases} \tag{4.1}$$

$I(t)$ is the afferent current charging the cell's membrane. When V crosses the threshold, a spike is emitted, and the depolarization is reset to V_r and kept constant for τ_{arp} milliseconds. If $I(t)$ is stationary, gaussian, and independent at different times (delta correlated), the distribution of the depolarization $P(V)$ and the mean emission rate ν are calculated to be (Fusi & Mattia, 1999)

$$P(V) = \frac{\nu}{\mu}\left[1 - exp\left(-2\frac{\mu}{\sigma^2}(\theta - V)\right)\right] \text{ for } V \in [0, \theta] \tag{4.2}$$

$$\nu \equiv \Phi(\mu, \sigma^2) = \left[\tau_{arp} + \frac{\sigma^2}{2\mu^2}\left(\frac{2\mu\theta}{\sigma^2} - 1 + e^{-\frac{2\mu\theta}{\sigma^2}}\right)\right]^{-1}, \tag{4.3}$$

for $V_r = 0$. The hypotheses on the statistics of the afferent current are quite well satisfied in a large spiking network (Amit & Brunel, 1997b). This model does not include adaptation effects, essential for fitting neural response dynamics of real cells (Rauch et al., 2002), limiting the increase in neural emission rates during sustained stimulation. In our simulations, this simplification is corrected by hand (see section 4.2.5).

4.2 The Learning Process.

4.2.1 The Network Architecture. The network (modeling a cortical module) is composed of N_E pyramidal cells and N_I interneurons. Each neuron receives, on average, C_E synaptic contacts from excitatory and C_I from inhibitory neurons inside the network and C_{ext} excitatory synaptic contacts

representing external afferents (Amit & Brunel, 1997b). The current resulting from the activation of the external synapses represents noise from the rest of the cortex and selective afferents due to stimuli.

When the network is set up, the afferent presynaptic neighbors of a given neuron are selected as follows: for each (postsynaptic) neuron (excitatory or inhibitory), one selects the presynaptic neighbors, independently and at random, by a binary process in which a presynaptic excitatory (inhibitory) neuron is a neighbor with probability C_E/N_E (C_I/N_I). The existing inhibitory as well as the excitatory synapses onto interneurons are assigned continuous values, each drawn from a gaussian distribution with its preassigned mean and variance. These synapses remain fixed throughout the simulation. The plastic excitatory-excitatory synapses (prior to training) are distributed independently and randomly, with $\mathcal{P}(J_{ij}(0) = J_p) = C_p^0 = 0.25$. This is equivalent to a distribution for excitatory-excitatory synapses with mean $J_{EE}/\theta = C_p^0 J_p + (1 - C_p^0)J_d = 0.022$ and variance $\Delta^2 J_{EE}/\theta^2 = C_p^0(1 - C_p^0)(J_p^2 + J_d^2) = 0.00063$. Numerical values correspond to the parameters in Table 1.

Furthermore, to each synapse is associated a transmission delay δ, which represents the time needed by the presynaptic spike to affect the postsynaptic depolarization. In our simulations, we chose $\delta = 1$ ms for all the synapses. This is the unstructured state of the network, which is supposed to sustain spontaneous activity. The complete list of parameters used in the simulations is reported in Table 1.

4.2.2 The Dynamics. The simulation consists of a numerical integration of the discretized dynamical equations of both neurons and plastic synapses. The temporal step Δt is chosen to be shorter than the time between two successive afferent spikes. In our simulations, we take $\Delta t = 0.05$ ms.

The initial distribution of depolarization in the network is set uniform. Spikes begin to be emitted due to external excitatory afferents. All neurons are receiving a nonselective external current $I_i^{(ext)} = J_{ext}\rho(t)$, where $\rho(t)$ is a Poisson process with mean $C_{ext}\nu_{ext}$ per unit time. ν_{ext} is taken of the order of the rate of excitatory neurons in the spontaneous state and is kept fixed. At each Δt, the afferent external current is $J_{ext}\rho(t)\Delta t$.

The initial distribution of the neural depolarization is found not to be important. The network reaches its stationary state (depending on the synaptic matrix and level of external signal) within short relaxation times (see Figure 6 and the discussion in section 5.1). The network is allowed to evolve freely (i.e., without stimulus presentation) for about 100 ms, to reach stationary spontaneous activity, and then the training stage begins.

The depolarization of all neurons is sequentially updated according to equation 4.1. If $V_j(t+\Delta t) > \theta$, a spike is delivered to all postsynaptic neurons, and the depolarization is reset to $V_j = V_r$. The spike adds to the value of the depolarization of postsynaptic neuron i, at time $t + \Delta t + \delta$, the value of the synaptic efficacy connecting the neuron j to i, if they are connected.

Table 1: Parameters Used in the Simulations.

Network parameters		
N_E Number of pyramidal cells		5000
N_I Number of interneurons		1250
C_E Number of recurrent E connections per cell		380
C_I Number of recurrent I connections per cell		120
C_{ext} Number of connections from outside		380
ν_{ext} [Hz] Spike rate at external synapses		5
p Number of selective populations		5
f Fraction of cells responding to a stimulus		0.1
Single cell parameters	E	I
$\theta[\theta]$ Spike emission threshold	1	1
V_r/θ Postspike reset potential	0	0
$\beta_I/\theta[\text{ms}^{-1}]$ Leakage current	.011	.0113
τ_{arp} [ms] Absolute refractory period	2	2
Synaptic parameters		
J_{ext}/θ EPSP produced by external afferent		.019
J_{EI}/θ IPSP amplitude on pyramidal cells		.063
J_{IE}/θ EPSP amplitude on interneurons		.025
J_{II}/θ IPSP amplitude on interneurons		.055
J_p/θ EPSP produced by potentiated synapse		.057
J_d/θ EPSP produced by depressed synapse		.01
C_p^0 Fraction of J_p in unstructured network		.25
δ [ms] Synaptic delay		1
Synaptic dynamics parameters		
θ_X Threshold for synaptic transition		.374
θ_1/θ Threshold for upregulation of X		.7
θ_2/θ Threshold for downregulation of X		.5
$\alpha[\text{ms}^{-1}]$ Drift toward 0		.0067
$\beta[\text{ms}^{-1}]$ Drift toward 1		.01
a Amplitude of up jump		.17
b Amplitude of down jump		.14

Notes: Units are given in brackets. Before structuring, the mean and variance of the excitatory efficacy in the excitatory population are given by $J_{EE}/\theta = C_p^0 J_p + (1 - C_p^0)J_d = 0.022$ and $\Delta^2 J_{EE}/\theta^2 = C_p^0(1 - C_p^0)(J_p^2 + J_d^2) = 0.00063$.

Moreover, if the emitting neuron is excitatory, all plastic synapses connecting it to other excitatory neurons are updated according to equations 3.1, 3.2, and 3.4. The level of the postsynaptic depolarization, determining the direction of the jump in $X(t)$ according to equation 3.4, is read at the time of the presynaptic emission (see section 3.1). If $X_{ij}(t + \Delta t)$ (the internal variable of the plastic synapse connecting neuron j to i) crosses the threshold θ_X, the efficacy $J_{ij}(t + \Delta t)$ is suitably modified, producing either LTP or LTD.

4.2.3 Statistics of Stimuli. The p stimuli to be used in training are set up when the simulation is initialized and is kept fixed. Each stimulus cor-

responds to a pool of fN_e, visually responsive excitatory neurons. f is the coding level of the stimuli and is chosen low ($f \ll 1$). These pools are selected nonoverlapping, that is, the neurons have a perfectly sharp tuning curve, and $pf < 1$. They are p consecutive groups of fN_e neurons. Although this is not a realistic constraint, it is very useful in allowing the monitoring of the complex double dynamics by mean-field theory and in simplifying greatly the analysis of the learning dynamics. This fact, however, does not render the process trivial (see section 5.1). Moreover, for low memory loading levels, $p \ll 1/f$, it is a good approximation to the case of unconstrained random choice of stimuli (Amit & Brunel, 1997b). At higher loading levels, one must confront the full issue of the network memory capacity, whose details are beyond this study.

The presentation of a stimulus is expressed by an increase in the rates of the external afferents to the selective cells (the corresponding pool). The rate of spikes arriving at these neurons is increased by a factor $g_e > 1$. $\rho_k(t)$ is still a Poisson process, but with mean $g_e C_{ext} \nu_{ext}\, dt$, where the index k runs over the visually responsive population. External currents to the other excitatory neurons are unaltered. Similarly, the afferents to all interneurons increase their activation rates by a factor $g_i > 1$ (Miller et al., 1996). Accordingly, the neurons selective to the stimulus presented emit at elevated rates. In other words, a stimulus elicits a visual response in the same subset of cells whenever it is presented. There is no noise in the process of presentation.

In a more realistic situation, the subset of cells excited may be slightly different on different presentations of the same stimulus. Accordingly, we carried out simulations with a noisy version of the stimuli. In these simulations, each stimulus was considered a prototype of specific fN_E cells. In each presentation, a fraction $1 - f_1$ of the prototype was excited, as well as f_2 of all other $(1 - f)N_E$ excitatory cells. f_1 is the noise level, and $f_1 = f_2 = 0$ is the noiseless case. To have a constant (on average) number of stimulated cells in each presentation, we chose f_2 so that

$$f_2 = f_1 f/(1 - f).$$

4.2.4 Training Protocol. For the training protocol, the set of stimuli is repeatedly presented to the network. Each stimulus appears for T_{stim} milliseconds. Then it is removed, and following a delay period of T_{delay}, during which none of the populations is stimulated, another stimulus is presented. The presentation sequence of the stimuli is either kept fixed ($1 \to \cdots \to p \to 1$) or the sequence is generated by choosing each stimulus to be presented, independently and randomly, with probability $1/p$. All along the simulation, during and between stimulus presentation, the neural and synaptic dynamics are free and are described by equations 3.4 and 4.1.

4.2.5 Control of Visual Response. As structuring takes place, the increasing average recurrent excitatory synaptic efficacy causes a significant in-

crease of neural emission rates, at parity of external signal (contrast, g_e). Such an increase is doubly undesirable—first, because it is not observed experimentally (Erickson & Desimone, 1999), and second, and more relevant for the present purposes, because it distorts the learning process. As things stand, it seems to be an artifact of the simplicity of the single cell dynamics as well as of the synaptic transmission model rather than of the learning process. In a more realistic situation, this problem is resolved by the adaptation features of the neurons and of the synaptic transmission (Tsodyks & Markram, 1997). This tendency of increased visual response during training is partially balanced by the stimulation of the inhibitory neurons during stimulus presentation. The enhanced firing of interneurons limits the visual response of the pyramidal cells by the hyperpolarizing currents. Moreover, it enhances the synaptic depression process between stimulated and unstimulated neurons because the stronger hyperpolarizing currents, arising from stimulated interneurons, decrease the mean depolarization level of neurons of the unstimulated population. This enhances the depression of synapses afferent on them. The stimulation of inhibitory neurons, and its effects, appears to be consistent with experimental findings (Steele & Mauk, 1999). However, the activity of the inhibitory population cannot grow beyond a certain level because the interneurons also inhibit each other. On the other hand, inhibitory contacts among interneurons cannot be weakened too much, or the emission rate of the inhibitory population becomes so high as to suppress the activity of the excitatory cells completely.

When inhibition was no longer sufficient, we artificially kept the rate of stimulated neurons approximately constant during the learning process. The emission rates during stimulus presentation are suggested by the properties of the single synapse (see section 3.2) and are chosen at the start of the simulation. When, as a consequence of synaptic structuring, these rates exceed the initial level by more than 15%, stimulus presentation is interrupted. The synaptic structuring reached is used to calculate, by mean-field analysis (see the appendix), a new level of contrast (g_e) for the stimuli, keeping g_i fixed. g_e is calculated to produce the original rate of visual response, and the simulation resumes.

4.2.6 Observables Monitored. During the simulation, various observables related to the collective neural activity as well as the synaptic dynamics are sampled. To describe the evolution of the structuring among excitatory neurons in the network, we define functional neural populations and functional synaptic populations. The neural populations are of excitatory neurons, such as the population corresponding to one of the p stimuli; when a particular stimulus is presented, the union of the $p-1$ populations corresponding to the other stimuli, not now recalled; and the population of background cells. In every phase of the simulation, the neurons in each of these populations receive the same average external input and see, on average, the same synaptic structure.

The functional synaptic populations are the synapses connecting pairs of neurons within a functional neural population or between two different functional neural populations. Therefore, a synaptic population is fully defined once the functional properties of its pre- and postsynaptic neurons are specified. The state of any synaptic population (its structuring) is quantified by the fraction, C_p, of potentiated synapses in that population.

In practice, we monitor only two structuring parameters, C_p. One of them is C_p^{HH}, between neurons in one of the p selective populations. It is one parameter and not p since we observe a very small variability of structuring corresponding to the different stimuli, and so we monitor their average. The other is C_p^{HL}, between neurons belonging to a selective population and those in the background or in other, unstimulated populations. Again, the average over p such populations is monitored. Recall that only synapses with high-rate presynaptic neurons have a significant transition probability.

We do not distinguish between postsynaptic neurons in the background and neurons of nonselected populations because their rates are rather close. This is obvious before the network is significantly structured. It remains so after structuring due to the enhanced inhibitory activity. Most of the (nonstimulated) neurons emit at very low rates, and the distributions of frequencies in those populations are quite similar. This was checked by carrying out a set of simulations and comparing the structuring of the synaptic population between visually responsive and background neurons with the structuring between visually responsive and neurons responsive to a different stimulus. Moreover, we do not consider the structuring between background, or unselected, neurons and other populations, because the presynaptic rates are low, and so structuring is negligible, as confirmed by the simulations.

Because the selective neural populations are nonoverlapping, the functional synaptic populations defined above are also nonoverlapping. This is true also for the synaptic populations between selected neurons and the rest, because even when the synapses of the two populations share postsynaptic neurons, the presynaptic neurons are different. The synaptic structuring reached in one synaptic population is not disrupted by the presentation of a different stimulus, and this fact simplifies the analysis of synaptic structuring.

The level of synaptic structuring required for WM states may be estimated by mean-field analysis (see the appendix). When synaptic structuring reaches the level theoretically estimated, the training stage is interrupted. Each stimulus is presented for 150 ms and then removed and the network evolves for 1 second in the absence of further stimulations. If, following the removal, the network exhibits a WM state for all stimuli, the learning stage is terminated. Otherwise, it is resumed. If stimulus presentation continues after WM activity appeared, the structuring reaches an asymptotic level and further presentations do not affect the synaptic matrix. The asymptotic

structuring level expresses a detailed balance between potentiating and depressing processes (see section 6.1).

5 Results

5.1 The Structuring Process. The simulations presented here are for nonoverlapping stimuli. The parameters are given in Table 1. Even in this basic case, the process of synaptic structuring, and the consequent appearance of WM states, is not trivial. Indeed, various instabilities tend to appear during learning. The most common instabilities encountered in our simulations were oscillatory behavior, uncontrolled growth of the network global activity, or depression where one expects potentiation or vice versa. The essential underlying reason is that to reach stable, selective WM states, synapses must not only be potentiated among visually selective neurons, but this potentiation must be accompanied by adequate depression from selective to nonselective cells (Brunel, 2000). On the other hand, with the synaptic dynamics proposed here, in any population of synapses, one finds potentiations as well as depressions, as we explain below.

Depressing synapses that should be potentiated can prevent the formation of WM states, because the fraction of potentiated synapses remains too low, at fixed J_p and J_d. Often these effects appear when the level of visual response becomes too high. As a consequence, the rate of synaptic modifications increases appreciably, and hence, the effects of unwanted synaptic transitions, occurring due to the wide distribution of rates inside the neural populations, are amplified. Alternatively, the ratio between the probabilities of potentiation and depression could vary, again provoking unwanted synaptic modifications.

Another source of unwanted plasticity is the correlation between the stimulated and the unstimulated pyramidal cells. Due to the increased inhibitory activity, the activity in the background population is quite low. The spike emission of a neuron belonging to the background population is provoked principally by the spikes afferent from the visually responsive population. As a consequence, spike emission in a presynaptic neuron of the selective population consistently tends to precede the emission of the postsynaptic neuron if it belongs to the background population (Rubin, Lee, & Sompolinsky, 2001). Thus, despite the low emission rate, the postsynaptic depolarization could be found often at a high level when the synapse is activated by presynaptic emission. This could provoke LTP instead of the appropriate LTD. However, this effect is negligible when the network is sufficiently large and the single EPSP is small with respect to the threshold for spike emission.

Hence, in a way, the results we report represent a demonstration that in the rich and complex space of parameters of the synapses and the neurons exists a zone in which the fundamental structuring for working memory can take place. It would have been more satisfactory had the scenario been

more robust, in the sense of self-organization, so that learning would induce neural activity conducive to structuring. But the complexity of the situation limits us to one step at a time.

Figure 3 reports the average fraction of potentiated synapses in both the HH and HL synaptic populations as a function of the number of presentations per stimulus. C_p increases monotonically in the HH populations with stimulus presentation, while the fraction of potentiated synapses decreases with stimulus presentation (in the HL populations). Figure 4 reports the average number (averaged over stimuli) of synaptic potentiations and depressions per presentation in both the HH and HL synaptic populations. Note that there are depressions in the HH populations as well as potentiations in the HL populations, due to the wide distribution of rates in each

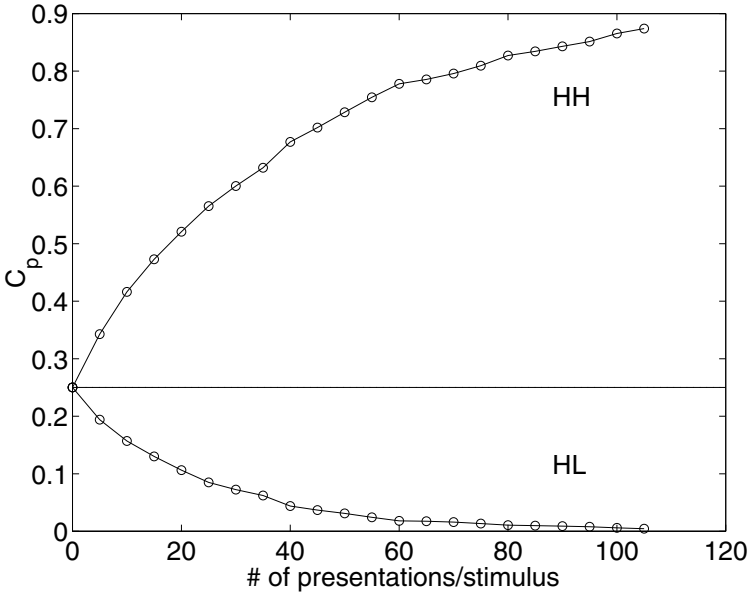

Figure 3: Synaptic structuring: C_p in the two monitored synaptic populations as a function of the number of presentations (nonoverlapping populations). Horizontal line: The unstructured initial state ($C_p^0 = 0.25$). C_p^{HH} (between visually responsive neurons) increases monotonically with stimulus presentation; C_p^{HL} (between visually responsive to nonresponsive neurons) decreases monotonically. The values of C_p^{HH} and C_p^{HL} are averaged over all functionally equivalent synaptic populations. The interpopulation variability is included in the circles representing the points. Synaptic structuring allowing for WM is reached after 105 presentations of each stimulus. See also Figure 7. The parameters are given in Table 1.

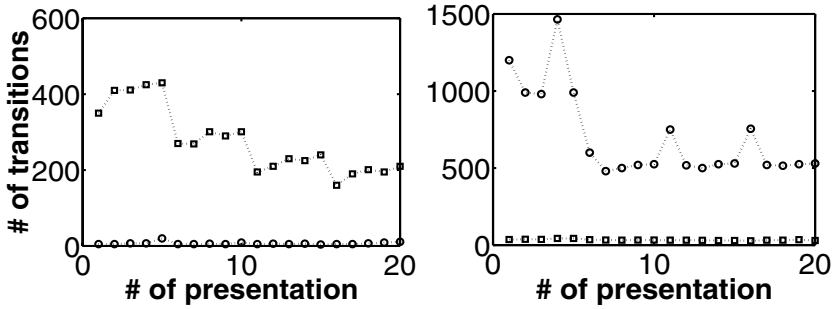

Figure 4: Number of synaptic transitions (stimulus average) per presentation versus presentation number for the first 20 presentations. Squares represent number of potentiations and circles the number of depressions. (Left) HH population: number of potentiations greater than the number of depressions. (Right) HL population: number of depressions greater than the number of potentiations. The difference between the absolute numbers of transitions in the two figures is due to the greater number of synapses in the HL population. Parameters are as in Figure 3.

population (see Figure 5), which produces a finite probability that synapses within a selective population of neurons find a high-rate presynaptic neuron and a low-rate postsynaptic neuron. Similarly, there is a finite probability that synapses between selective and nonselective populations find two high-rate neurons. However, with the parameters of Table 1 and the relevant rates, the number of "correct" transitions is overwhelmingly greater than the number of "wrong" transitions. The outcome is an increase of C_p^{HH} and a strengthening of the mean synaptic efficacy among selective neurons and a monotonic decrease of C_p^{HL} and a depression of the mean synaptic efficacy from selective to nonselective neurons. In this situation, we recover the classical Hebb rule.

As a control, we have verified that similar results are obtained when the set of stimuli is noisy. We carried out simulations with $f_1 = 0.1$ and $f_1 = 0.2$. Recall that $1 - f_1$ is the probability that a neuron of the prototype is effectively activated by its presentation in the presence of noise. The only noticeable, and expected, effect was that WM states require more presentations to appear: 140 to 150 presentations per stimulus instead of 100 to 110 required in the noiseless case.

5.1.1 Appearance of Working Memory. Working memory (selective delay activity) states appear for $C_p^{HH} = 0.875$ and $C_p^{HL} = 0.0045$. The appearance of WM states is related not only to the level of synaptic structuring, that is, the values of C_p in the various synaptic populations, but also to the other

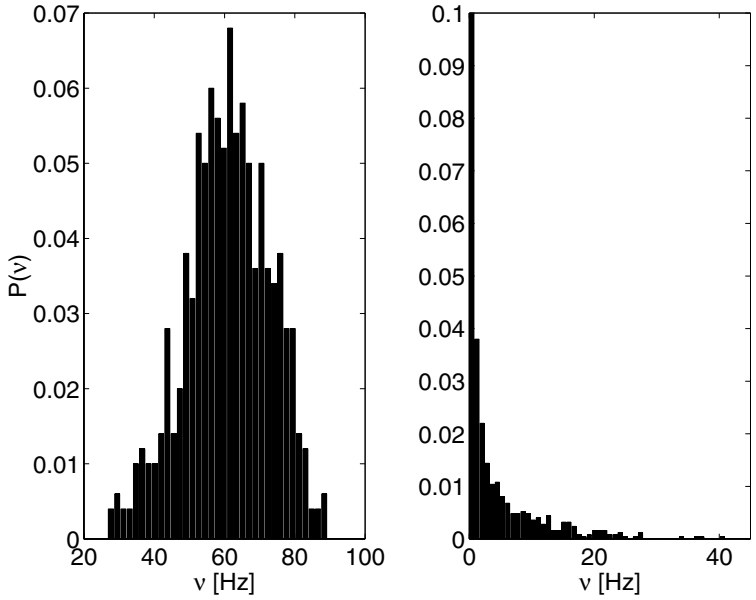

Figure 5: Population distribution of spike rates during stimulation. (Left) Stimulated population. The mean emission rate is $\nu_{stim} = 60$ Hz. (Right) Unstimulated pyramidal cells; the mean emission rate is $\nu_{bg} = 0.9$ Hz. Despite the low mean emission rate, neurons are found with high rate. Note that the high-frequency tail of the background distribution overlaps with the stimulated distribution. This could impair the synaptic structuring. Recurrent inhibition is effective in reducing this overlap. See the text for details.

parameters of the network, principally the ratio J_p/J_d between potentiated and depressed synaptic efficacy. For example, decreasing J_p once the structuring level allowing for WM states is reached prevents the appearance of WM states. On the other hand, increasing J_p could destabilize spontaneous activity. All network parameters, as connectivity, mean synaptic efficacies, level of synaptic structuring for WM states, and so forth should be chosen to lie in a biologically plausible range.

Starting from an unstructured synaptic matrix ($C_p^0 = 0.25$), 100 to 150 presentations per stimulus are required to reach stable WM, that is, selective delay states. Figure 6 shows the neural activity in a visually responsive population before, during, and following the presentation of a stimulus at various level of synaptic structuring. What is plotted is the number of spikes emitted per neuron, in bins of 5 ms, averaged over the selective populations and normalized to Hz (dividing by the bin size). The transients into the various stationary states, spontaneous activity, WM, or stimulated state are

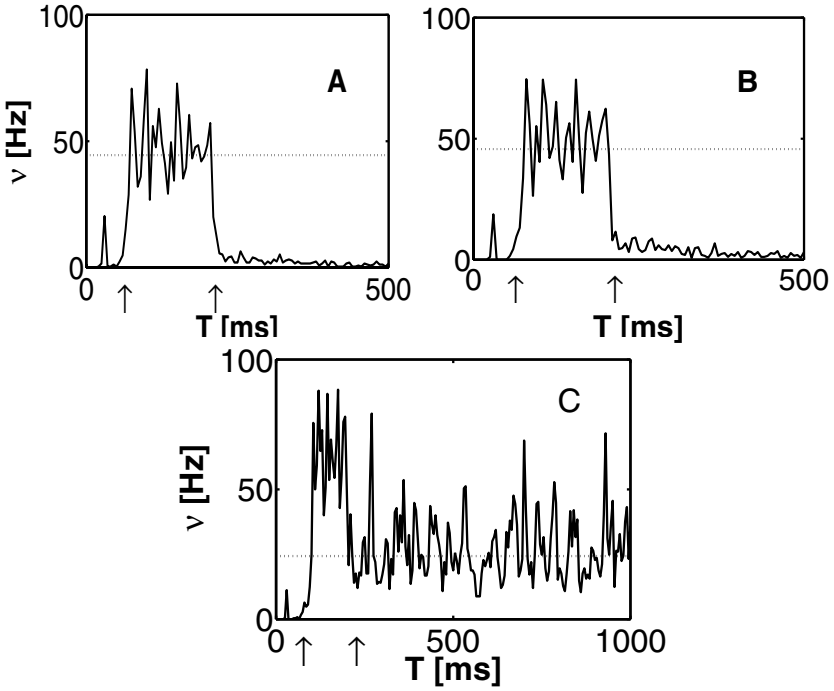

Figure 6: Selective population activity during trial at three structuring stages: population-averaged neural activity (in 5 ms bins) converted to Hz (see text), before, during, and following stimulation. Arrows indicate 150 ms stimulation interval. Note the short transients from one stationary state to another. Mean field predictions of mean emission rates, ν_{th}, during stimulation (ST), spontaneous (SA), and working memory (WM) activity are compared with the results of the simulation. (A) Fifty-five presentations per stimulus; $C_p^{HH} = 0.755$; $C_p^{HL} = 0.0245$. ST: $\nu_{th} = 51.5$ Hz $\nu_{sim} = 44.5 \pm 1.5$ Hz; SA: $\nu_{th} = 1.3$ Hz $\nu_{sim} = 1.21 \pm 0.21$ Hz. (B) Seventy presentations per stimulus; $C_p^{HH} = 0.8$; $C_p^{HL} = 0.016$. ST: $\nu_{th} = 51.5$ Hz $\nu_{sim} = 45.7 \pm 2.9$ Hz; SA: $\nu_{th} = 1.3$ Hz $\nu_{sim} = 1.17 \pm 0.18$ Hz. Horizontal dashed line: Average emission rate during stimulus presentation and SA. In both *A* and *B* no WM: population returns to spontaneous state after removal of stimulus. (C) Appearance of WM state: 105 presentations per stimulus; $C_p^{HH} = 0.875$ and $C_p^{HL} = 0.0045$. WM: $\nu_{th} = 27$ Hz $\nu_{sim} = 24.3 \pm 4.25$ Hz. Horizontal dashed line: Average emission rate during WM activity. Large fluctuations are due to strong finite-size effects. See text for details.

short, on the order of 50 to 100 ms. In Figures 6A and 6B, the level of synaptic structuring is still too low, and the stimulated population returns to spontaneous activity when the stimulus is removed. In Figure 6C, one observes a WM state in which the cells of the selective populations emit at elevated rates (24.3 Hz) following the removal of the stimulus. Mean field predictions for the mean emission rates during spontaneous and WM activity (dashed horizontal lines) are in good agreement with the simulations.

During WM activity, we observed very large fluctuations of the average emission rate. This is due to finite size effects; to reduce the duration of the simulations with the double dynamics, the selective populations were taken relatively small and, given the low connectivity, a neuron receives only about 38 connections from other neurons in the same selective population (see Table 1). Due to the small number of connections from other selective cells and the stochastic nature of spike emission, the current afferent on a cell has large fluctuations (of relative order $1/\sqrt{N}$, N is the number of pre-synaptic neurons) around its mean which produce fluctuations in the emission rate.

6 Estimates of the Structuring Process

6.1 Population Dynamics of the Structuring Level. We define q_+ as the probability that a depressed synapse undergoes LTP during one stimulus presentation and q_- as the probability of depression of a potentiated synapse per presentation. It is expected that $q_+ > q_-$ in an HH synaptic population and vice versa in an HL population. The fraction of potentiated synapses follows a population evolution as a function of the number of stimulus presentations,

$$C_p(n+1) = C_p(n)[1 - q_-(n)] + q_+(n)[1 - C_p(n)], \tag{6.1}$$

where $C_p(n)$ represents the fraction of potentiated synapses in a given synaptic population after n presentations of the same stimulus. The dependence of q_+ and q_- on n takes into account the possibility that they could vary along the learning process.

If both the frequencies of visual response and the statistics of the emission process do not vary appreciably during learning, q_+ and q_- would remain approximately constant. In this case, for nonoverlapping populations, after a large number of presentations,

$$\begin{cases} C_p^{HH} = q_+^{HH}/(q_+^{HH} + q_-^{HH}) & \text{for HH populations} \\ C_p^{HL} = q_+^{HL}/(q_+^{HL} + q_-^{HL}) & \text{for HL populations.} \end{cases} \tag{6.2}$$

Note that when the selective populations overlap, the structuring of a given population could change even if its preferred stimulus is not presented. In

this case, equation 6.1 becomes more complicated, and one must also take into account the structuring due to the presentation of different stimuli. We do not expand on this issue here.

In our case (see, e.g., Figure 4), the number of wrong transitions—depressions instead of potentiations in the selective population and potentiation between selective and nonselective—is rather small. We neglect these transitions, and equation 6.1 becomes

$$\begin{cases} C_p(n+1) = C_p(n) + q_+(n)[1 - C_p(n)] & \text{for HH populations} \\ C_p(n+1) = C_p(n)[1 - q_-(n)] & \text{for HL populations.} \end{cases} \tag{6.3}$$

The dashed curves in Figure 7 are a least-square fit of C_p in the HH and HL populations measured in the simulation by the solution of equation 6.3 with constant q_+ and q_-, during the first 20 stimulations. The degree of agreement between the curves indicates that these probabilities are approximately constant during learning, partly because the rates under stimulation are kept approximately constant.

6.2 Population Transition Probabilities and Transition Numbers. The probability of an LTP transition in a homogeneous population of synapses, per stimulus presentation of duration T, could be estimated as follows.[3] Let c be the probability of a synaptic contact from a neuron in the presynaptic population to a neuron in the postsynaptic one. The population of synapses connects neurons in two populations: one of N_{pre} presynaptic neurons and one of N_{post} postsynaptic ones (the physical neurons in the two populations can, of course, be the same). The number of potentiations in such a synaptic population, per presentation of a stimulus, is a random variable,

$$N_{pot} = \sum_{i,j} c_{ij} \cdot \gamma_{ij},$$

where the index j runs over the presynaptic neurons and i over the postsynaptic ones. If there exists a synapse between the two neurons, $c_{ij} = 1$, otherwise $= 0$. $\gamma_{ij} = 1$ if the synapse was potentiated during the stimulation, otherwise $= 0$. Hence, $\gamma_{ij} = 1$ with probability $P_{LTP}(\nu_i, \nu_j, T) \cdot \delta(J_{ij} - J_d)$, where J_{ij} is the synaptic efficacy before the stimulation and $\delta(\cdot)$ is 1 if its argument is zero, and zero otherwise. The mean number of potentiations is

$$\overline{N_{pot}} = \sum_{i,j} c_{ij}\delta(J_{ij} - J_d) \cdot P_{LTP}(\nu_i, \nu_j, T). \tag{6.4}$$

The sum on the right-hand side can be converted to a sum over pairs of activity (ν_i, ν_j). Let $P_{post(pre)}(\nu)$ be the probability of finding a neuron with

[3] The reasoning is analogous for LTD.

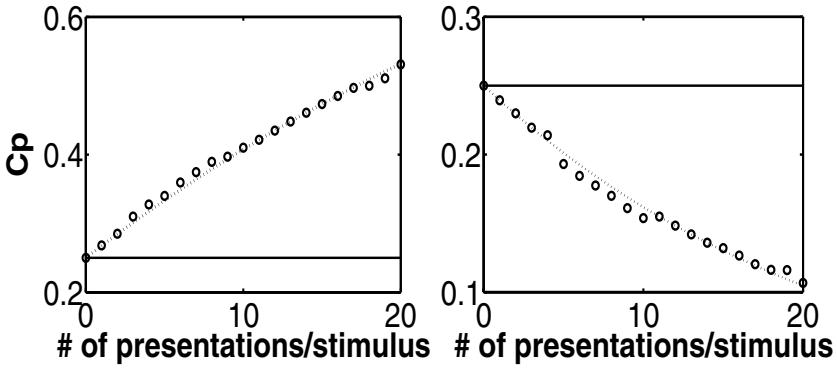

Figure 7: Population dynamics description of synaptic structuring during initial 20 presentations per stimulus. (Left) Average C_p in HH populations. (Right) Average C_p in HL populations. Dashed lines represent the solution of equation 6.3, with $q_+ = 0.0233$ and $q_- = 0.0426$, constant (independent of n). Error bars are included in the circles. Horizontal lines: unstructured state of the network.

rate ν in the post-(pre-)synaptic neural neural population, respectively. The probability of having a depressed synapse with a presynaptic neuron at rate ν_j afferent on a postsynaptic neuron at rate ν_i is $c(1-C_p)P_{pre}(\nu_j)P_{post}(\nu_i)$. Hence, when the number of neurons is large, equation 6.4 becomes

$$\overline{N_{pot}} \simeq c(1-C_p)N_{pre}N_{post} \int\int d\nu_i\, d\nu_j P_{LTP}(\nu_i, \nu_j, T)P_{pre}(\nu_j)P_{post}(\nu_i). \quad (6.5)$$

Correspondingly, the mean number of synaptic depressions is

$$\overline{N_{dep}} \simeq cC_pN_{pre}N_{post} \int\int d\nu_i\, d\nu_j P_{LTD}(\nu_i, \nu_j, T)P_{pre}(\nu_j)P_{post}(\nu_i). \quad (6.6)$$

If during learning, the integrals on the right-hand side of equations 6.5 and 6.6 do not vary significantly, they can be identified, respectively, with q_+ and q_-. In that case, it becomes straightforward to obtain equations 6.3 from equations 6.5 and 6.6.

In order to compare the theoretical estimates with the values of q_+ and q_- obtained from simulations, we have to estimate P_{LTP} and P_{LTD} over the range of frequencies observed in the simulation. For P_{LTP}, the rate intervals of both pre- and postsynaptic activity cover the distribution in the stimulated population. Similarly, for P_{LTD}, ν_{pre} varies over the emission rates of stimulated neurons, while ν_{post} varies over the rates of unstimulated neurons. (See, e.g., Figure 5.)

To obtain the currents giving rise to the observed emission rates, we proceeded as follows. In the stimulated population, the neurons operate in a signal-dominated regime (Fusi & Mattia, 1999), with small fluctuations. We

assume that the variance of the current is constant within the population and is given by mean-field analysis (see the appendix). The mean current corresponding to a given frequency is simply obtained (for constant σ) by inverting the transduction function, equation 4.3, which is a monotonic function of μ. In the unstimulated population, the neurons operate in the noise-dominated regime (Fusi & Mattia, 1999); spike emission is due to sporadic large fluctuations in the afferent current, which tends to hyperpolarize the membrane. Mean emission rates are very low, and the corresponding population distribution of rates is peaked around the mean-field result. We assume that all neurons in the population are in this state of activity. Mean field then provides the mean and variance of the currents.

We proceed by simulating the coupled neural and synaptic dynamics, as described in Fusi et al. (2000), to obtain P_{LTP} and P_{LTD}. The extent to which the assumptions used are justified in the real network can be judged by comparing the theoretical estimates, equations 6.5 and 6.6, and the probabilities observed during the simulation: $q_+^{th} = 0.017$ and $q_+^{sim} = 0.023 \pm 0.005$, while for LTD we have $q_-^{th} = 0.038$ and $q_-^{sim} = 0.043 \pm 0.009$.

6.3 Estimating Lifetime of Synaptic Structure. The synaptic structure may be affected by synaptic transitions provoked by spontaneous or selective delay activity. This may cause progressive erasure of the stored memories in the absence of stimulation. The mean lifetime of the acquired synaptic structure depends on the probability of having such synaptic transitions. After stable WM states appeared, a separate set of simulations was carried out in order to check the stability of the synaptic structure against both spontaneous and selective delay activity. First, we checked the stability of the synaptic structure when the network exhibits spontaneous activity. Simulations as long as 60 seconds were carried out, with no stimulation. There were no modifications in synaptic matrix. Similarly, a WM state was elicited by presenting the corresponding stimulus for 150 ms, and the network evolved freely for 4 seconds. The time difference with respect to the case of the spontaneous activity is due to the shorter lifetime of the WM state as a consequence of finite-size effects. Again, there were no synaptic modifications.

The probability of a synaptic transition during spontaneous activity is very small, because the average rate of about 1 Hz $\ll 1/\tau_p$. Thus, the number of repetitions needed to obtain a reasonable estimate of these probabilities becomes enormous. To obtain a rough estimate of q in spontaneous activity, we ran simulations to obtain the P_{LTP} for neurons at a rate of 20 Hz and then rescaled this probability to rates of 1 Hz. To obtain the first, we ran 10^6 repetitions of the single synapse simulation, of $T = 400$ ms each, with $\nu_{pre} \equiv \nu_{post} = 20$ Hz. No transition occurred. The default estimate of the transition probability is then $P_{LTP}(20, 20, T = 400) \sim 10^{-6}$. In other words, the mean time one has to wait until the synapse makes a spontaneous transition (at 20 Hz) is about 4 days. Next we approximately rescale this probability to 1 Hz.

For n up-jumps to provoke LTP within a time interval T', one must have,

$$na - \beta T' \geq \theta_X, \tag{6.7}$$

where a is the single up-jump amplitude and β is the synaptic refresh current (see equations 3.2 and 3.4). For n fixed, the longest time interval within which the presynaptic spikes must arrive and yet be able to produce LTP is $T_{\max}(n) = (na - \theta_X)/\beta$. For the parameters of Table 1, three spikes, all provoking up-jump, within 20 ms is the most probable burst that can produce LTP, considering the low emission rates of both pre- and postsynaptic neurons. Hence, to provoke the transition, such a burst must occur within the 400 milliseconds over which we have measured the transition probabilities above. During spontaneous activity, the statistics of the emission process of the neurons is well approximated by a Poisson process (Amit & Brunel, 1997b), then

$$P_3(T' = 20; \nu = 20) \leq 20^3 \cdot P_3(T' = 20; \nu = 1),$$

where $P_n(T'; \nu)$ is the probability that n presynaptic spikes occur within a time interval T' when the emission rate is ν. Neglecting other factors, as the dependence of the probability of an up-jump on the postsynaptic emission rate, we obtain

$$q_{SA}(400) = P_{LTP}(1, 1, 400) \sim 20^{-3} P_{LTP}(20, 20, 400),$$

leading to a mean lifetime of the order of 10 years.

7 Discussion

The principal result of this study is a feasibility test. The spike-driven synaptic dynamics, introduced in Fusi et al. (2000), for a suitable choice of the parameters implements rate-dependent plasticity and exhibits both long-term potentiation and long-term homosynaptic depression under diverse experimental stimulation protocols. [4] It is not to be excluded that a synaptic device in natural conditions behaves more like the synapse discussed here than as in the special protocols in which precise timing is observed.

Moreover, leaving from an unstructured synaptic state, the synaptic dynamics is able to drive the network into a structured state, sustaining selective delay activity, or working memory. The generated synaptic structure is robust against spontaneous and delay activity in the absence of stimulation. The question of stability of the acquired synaptic structure, and hence the related neural activity, is also addressed.

The appearance of WM states, following the repetitive presentation of a set of stimuli, is not simply a direct consequence of the rate-dependent

[4] This synaptic dynamics does not generate long-term heterosynaptic depression.

plasticity, implemented by the synaptic model. Several constraints must be met during the structuring stage:

- The effects of LTP should be adequately balanced by LTD to avoid instabilities along the learning process. This balance between the probabilities of LTP and LTD, imposes constraints on the synaptic and neural parameters. Further work is needed to relate such constraints to the neural and synaptic parameters in a simple form.
- The frequency distributions in the stimulated and unstimulated populations should not overlap significantly. Alternatively, the synapse should be highly sensitive to small variations of the frequencies in the overlap region (Del Giudice & Mattia, 2001). Indeed, this could be a source of unwanted plasticity that in turn impairs the structuring process. We have found that recurrent inhibition could play a significant role in separating the distributions, reducing the high-rate tail of the frequency distribution of the unstimulated populations.

A significant by-product, mentioned here only briefly, is the resulting extension of the Hebbian plasticity rule. A realistic synaptic model would generate both LTP as well as LTD in any population of synapses. In the particular situation (parameters) considered in detail here, the difference between "right" and "wrong" transitions is so large that the classical Hebbian picture ensues. But when one deals with the emergent coupling between two neural populations whose mean rates are not so different (as between stimulus driven cells and delay activity cells), the extension of the Hebbian scenario promises saturation in structuring, which is an essential ingredient in maintaining independent representations alongside WM.

7.1 Back to Timing-Dependent Plasticity. The sharp cutoff in the time difference between the arrival of pre- and postsynaptic spike, observed in experiment (Bi & Poo, 1998), could be a consequence of the experimental procedure. In the model presented here, the two thresholds (see equation 3.4) can be chosen to reproduce the results of Markram et al. (1997) when the two neurons connected by the synapse operate in deterministic conditions. This may, in fact, be the case in the experiments mentioned.

In a deterministic situation, one can consider the two neurons stimulated by a constant noiseless current. The evolution of the depolarization is deterministic. Thus, there is a relation between the value of V at a given instant and the time elapsed from the emission of the last spike. If one chooses the two synaptic thresholds θ_1 and θ_2 of equation 3.4 to be

$$\theta_1 = \theta - T_1\mu, \qquad \theta_2 = T_2\mu, \tag{7.1}$$

where μ is the total current, the following picture emerges. Upon the emission of a presynaptic spike, the postsynaptic neuron has $V < \theta_2$ only if it

emitted a spike at most T_2 before, and the synaptic activation causes downregulation. Similarly, the postsynaptic neuron has $V > \theta_1$ only if the time of the presynaptic spike emission precedes the postsynaptic spike by at most T_1. It will then be followed by an upregulation of the synapse. If this is the case, one should conclude that up- and downregulation depend on the level of postsynaptic depolarization and the timing effect is only a consequence of the experimental setup, as argued above. Recent experimental findings seem to corroborate this hypothesis (Sjöström et al., 2001).

Recently, Abbott and Song (1999) and Rubin et al. (2001) studied the behavior of a synaptic model into which the exact temporal relation, observed experimentally by Bi & Poo (1998), is built in. Efficacy is modified according to the temporal interval $\Delta t = t_{post} - t_{pre}$, where t_{pre} and t_{post} are the times of the pre- and postsynaptic spike emission. When $\Delta t > 0$, efficacy is upregulated, and the efficacy is downregulated for $\Delta t < 0$.

Such a synaptic mechanism tends to potentiate synapses connecting correlated neurons, for example, a presynaptic neuron that consistently fires before the postsynaptic one. On the other hand, presynaptic inputs that are not causally correlated with postsynaptic firing are weakened. The overall effect is the convergence of the synaptic distribution to an asymptotic stationary distribution. Depending on the update rule, the equilibrium distribution can be either unimodal or bimodal (Rubin et al., 2001). However, in both cases, the asymptotic distribution is largely insensitive to the firing rates of pre- and postsynaptic cells. Therefore, such a model of plastic synapse is unable to structure the synaptic matrix to sustain selective delay activity.

7.2 Open Issues. The collective behavior of coupled homogeneous neural and synaptic populations has been described in a compact form, in terms of probabilities of potentiation P_{LTP} and depression P_{LTD}, functions of the pre- and postsynaptic emission rates. Here, these functions were obtained from the detailed model of the plastic synapse. It is not clear whether such a description could be more general, so as to be qualitatively independent of the detailed neural and synaptic dynamics. A priori, this seems plausible as a general consequence of the stochasticity of the neural activity. If so, we could characterize the properties of P_{LTP} and P_{LTD}, allowing for successful structuring, regardless of the specific model of the synapse. Of course, the construction of a detailed synaptic model, which matches both available experimental data and theoretical desiderata, should be the natural conclusion of such a study.

The constraints on the transition probabilities become tighter when the issue of network capacity is considered. If stimuli are sparsely coded ($f \ll 1$) and the probabilities of transition are low (slow learning), a necessary condition to recover the optimal storage capacity is that the number of potentiations approximately balances the number of depressions in each presentation, requiring $q_- \sim f q_+$ (Amit & Fusi, 1994; Brunel, Carusi, & Fusi,

1998). This ensures that the difference between C_p in HH populations and C_p in HL populations, reached asymptotically, is maximal, depending on the number of stimuli to be learned. However, the appearance of WM states is not guaranteed. It depends not only on the level of structuring but also on the other network parameters. It remains to be seen whether the network exhibits WM activity in a biologically plausible range of parameters. The behavior of the synaptic device is manipulable. By choosing suitably the parameters a, b, α, β, and θ_X, the balance constraint may be satisfied. Simulations should be carried out to check the behavior of large networks at high loading level. Those require very efficient algorithms, such as Mattia and Del Giudice (2000).

But little is guaranteed; the results reported in Amit and Fusi (1994) and Brunel et al. (1998) are obtained under a simplifying hypothesis: the neurons are binary, and the existence of the attractors is checked by using a signal-to-noise ratio analysis. A further step toward the networks of spiking neurons is made by Herz and colleagues (see for a review Herz, 1996). They studied the capacity of network with analog neurons (no spiking) but with a symmetric connectivity matrix. The situation may be quite different when one deals with a recurrent network of spiking neurons, like that studied here.

Appendix: Mean Field for Nonoverlapping Populations

The mean-field analysis developed allows calculating the mean firing frequencies in each of the populations in stationary (asynchronous) states of the network as a function of the instantaneous synaptic structure and the level of the external signal. The instantaneous synaptic structuring is described by the fraction of potentiated synapses in the various synaptic populations. Plastic synapses are divided by an incoming stimulus in three homogeneous populations, according to pre- and postsynaptic activities:

- **High pre- and postsynaptic activity.** It is expected that in this population, the fraction of potentiated synapses increases to $C_p^{HH} (> C_p^0)$.
- **High presynaptic and low postsynaptic activity.** The fraction of potentiated synapses decreases to $C_p^{HL} (< C_p^0)$.
- **Low presynaptic activity.** The probability of a synaptic transition is negligible; thus, the fraction of potentiated synapses is unaltered.

Following the presentation of a stimulus that has been previously "learned," the network divides in four functionally different populations of cells: cells belonging to the population activated by the stimulus (denoted *sel*); cells representing other stimuli, not activated (denoted +); cells not responsive to any stimulus (denoted *bg*); and interneurons (denoted *I*).

The mean firing rates in each in the four neural populations are given by mean-field equations (Amit & Brunel, 1997a),

$$\nu_{sel} = \Phi(\mu_{sel}, \sigma^2_{sel}),\ \nu_+ = \Phi(\mu_+, \sigma^2_+),\ \nu_{bg} = \Phi(\mu_{bg}, \sigma^2_{bg}),\ \nu_I = \Phi(\mu_I, \sigma^2_I).$$

The statistics of the afferent currents is calculated as function of synaptic structuring. The recurrent currents are

$$\begin{aligned}
\mu_{sel} &= -\beta_I^{(e)} + C_E[fJ_+\nu_{sel} + f(p-1)J_-\nu_+ + (1-fp)J_0\nu_{bg}] - C_IJ_{EI}\nu_I \\
\mu_+ &= -\beta_I^{(e)} + C_E[fJ_-\nu_{sel} + f[J_+ + (p-2)J_-]\nu_+ + (1-fp)J_0\nu_{bg}] - C_IJ_{EI}\nu_I \\
\mu_{bg} &= -\beta_I^{(e)} + C_E[fJ_-\nu_{sel} + f(p-1)J_-\nu_+ + (1-fp)J_0\nu_{bg}] - C_IJ_{EI}\nu_I \\
\mu_I &= -\beta_I^{(i)} + C_EJ_{IE}[f\nu_{sel} + f(p-1)\nu_+ + (1-fp)\nu_{bg}] - C_IJ_{II}\nu_I, \quad \text{(A.1)}
\end{aligned}$$

where

$$\begin{aligned}
J_+ &= C_p^{HH}J_p + (1 - C_p^{HH})J_d \\
J_- &= C_p^{HL}J_p + (1 - C_p^{HL})J_d \\
J_0 &= C_p^0 J_p + (1 - C_p^0)J_d. \quad \text{(A.2)}
\end{aligned}$$

The variances of the recurrent currents are

$$\begin{aligned}
\sigma^2_{sel} &= C_E[f\Delta J_+\nu_{sel} + f(p-1)\Delta J_-\nu_+ + (1-fp)\Delta J_0\nu_{bg}] + C_IJ^2_{EI}\nu_I \\
\sigma^2_+ &= C_E[f\Delta J - \nu_{sel} + f[\Delta J_+ + (p-2)\Delta J_-]\nu_+ + (1-fp)\Delta J_0\nu_{bg}] + C_IJ^2_{EI}\nu_I \\
\sigma^2_{bg} &= C_E[f\Delta J_-\nu_{sel} + f(p-1)\Delta J_-\nu_+ + (1-fp)\Delta J_0\nu_{bg}] + C_IJ^2_{EI}\nu_I \\
\sigma^2_I &= C_EJ^2_{IE}[f\nu_{sel} + f(p-1)\nu_+ + (1-fp)\nu_{bg}] + C_IJ^2_{II}\nu_I
\end{aligned}$$

where

$$\Delta J_+ = C_p^{HH}J_p^2 + (1 - C_p^{HH})J_d^2$$

and analogous for ΔJ_-, ΔJ_0. The external currents depend on the level of the external signal:

$$\begin{aligned}
\mu^{(ext)}_{sel} &= g_eC_{ext}J_{ext}\nu_{ext},\ {\sigma^{(ext)}_{sel}}^2 = g_eC_{ext}J^2_{ext}\nu_{ext} \\
\mu^{(ext)}_+ \equiv \mu^{(ext)}_{bg} &= C_{ext}J_{ext}\nu_{ext},\ {\sigma^{(ext)}_+}^2 \equiv {\sigma^{(ext)}_{bg}}^2 = C_{ext}J^2_{ext}\nu_{ext} \\
\mu^{(ext)}_I &= g_iC_{ext}J_{ext}\nu_{ext},\ {\sigma^{(ext)}_I}^2 = g_iC_{ext}J^2_{ext}\nu_{ext}.
\end{aligned}$$

In a steady state, the density function of V will be also stationary. It is given by equation 4.2. Both the mean and the variance of the afferent

currents are a linear function of v; hence, $P(V)$ is parameterized only by the mean emission rates. In other words, there is a one-to-one correspondence between the emission rates and the distribution of the depolarization.

Here we use the theory to determine (1) the range of C_p^{HH} and C_p^{HL} for which the network is able to sustain selective delay activity states and (2) the mean emission rate of stimulated populations as a function of the instantaneous level of synaptic structuring (3) and to compare simulation results in stationary states with theory.

Acknowledgments

We thank Stefano Fusi for having brought to our attention Sjöström et al. (2001). This study was supported by a Center of Excellence grant, "Changing Your Mind," from the Israel Science Foundation and by a Center of Excellence grant, "Statistical Mechanics and Complexity," of the INFM, Rome.

References

Abbott, L. F., & Song, S. (1999). Temporally asymmetric Hebbian learning and neuronal response variability. In M. S. Kearns, S. A. Solla, & D. A. Cohn (Eds.), *Advances in neural information processing systems, 11*. Cambridge, MA: MIT Press.

Amit, D. J. (1995). The Hebbian paradigm reintegrated: Local reverberations as internal representations. *Behavioral and Brain Sciences, 18*, 617–626.

Amit, D. J. (1998). Simulation in neurobiology—Theory or experiment? *TINS, 21*, 231–237.

Amit, D. J., & Brunel, N. (1997a). Model of global spontaneous activity and local structured activity during delay periods in the cerebral cortex. *Cerebral Cortex, 7*, 237–252.

Amit, D. J., & Brunel, N. (1997b). Dynamics of a recurrent network of spiking neurons before and following learning. *Network: Computation in Neural Systems, 8*, 373–404.

Amit, D. J., & Fusi, S. (1994). Learning in neural networks with material synapses. *Neural Computation, 6*, 957–982.

Bear, M. F. (1996). A synaptic basis for memory storage in the cerebral cortex. *Proc. Natl. Sci. USA, 93*, 13453–13459.

Bi, G. Q., & Poo, M. M. (1998). Synaptic modifications in cultured hippocampal neurons: Dependence on spike timing, synaptic strength and cell type. *Journal of Neuroscience, 18*, 10464–10472.

Brunel, N. (1996). Hebbian learning of context in recurrent neural networks. *Neural Computation, 8*, 1677–1710.

Brunel, N. (2000). Persistent activity and the single cell f-I curve in a cortical network model. *Network, 11*, 261–280.

Brunel, N., Carusi, F., & Fusi, S. (1998). Slow stochastic Hebbian learning of classes of stimuli in a recurrent neural network. *Network, 9*, 123–152.

Compte, A., Brunel, N., Goldman-Rakic, P. S., & Wang, X. J. (2000). Synaptic mechanisms and neural dynamics underlying spatial working memory in a cortical network model. *Cerebral Cortex, 10*, 910–923.

Del Giudice, P., & Mattia, M. (2001). Long and short-term synaptic plasticity and the formation of working memory: A case study. *Neurocomputing, 38*, 1175–1180.

Dudek, S. M., & Bear, M. F. (1992). Homosynaptic long-term depression in area CA1 of hippocampus and effects of NMDA receptor blockade. *Proc. Natl. Sci. USA, 89*, 4363–4367.

Dudek, S. M., & Bear, M. F. (1993). Bidirectional long-term modification of synaptic effectiveness in the adult and immature hippocampus. *Journal of Neuroscience, 13*, 2910–2918.

Erickson, C. A., & Desimone, R. (1999). Responses of macaque perirhinal neurons during and after visual stimulus association learning. *Journal of Neuroscience, 23*, 10404–10416.

Fusi, S., & Mattia, M. (1999). Collective behavior of networks with linear (VLSI) integrate-and-fire neurons. *Neural Computation, 11*, 643–652.

Fusi, S., Annunziato, M., Badoni, D., Salamon, A., & Amit, D. J. (2000). Spike-driven synaptic plasticity: Theory, simulation, VLSI implementation. *Neural Computation, 12*, 2227–2258.

Herz, A. V. M. (1996). Global analysis of recurrent neural networks. In E. Domany, J. L. van Hemm, & K. Schulten (Eds.), *Models of neural networks III*. New York: Springer-Verlag.

Kritzer, M. F., & Goldman-Rakic, P. S. (1995). Intrinsic circuit organization of the major layers and sublayers of the dorsolateral prefrontal cortex in the rhesus monkey. *Journal of Computational Neurobiology, 359*, 131–143.

Markram, H., Lübke, J., Frotscher, M., & Sakmann, B. (1997). Regulation of synaptic efficacy by coincidence of postsynaptic APs and EPSPs. *Science, 275*, 213–215.

Mattia, M., & Del Giudice, P. (2000). Efficient event-driven simulation of large networks of spiking neurons and dynamical synapses. *Neural Computation, 12*, 2305–2329.

Miller, E. K., Erickson, C., & Desimone, R. (1996). Neural mechanism of working memory in prefrontal cortex of macaque. *Journal of Neuroscience, 16*, 5154–5167.

Miyashita, Y. (1988). Neural correlate of visual associate long-term memory in the primate temporal cortex. *Nature, 335*, 817–820.

Mongillo, G., & Amit, D. J. (2001a). Spike driven synaptic dynamics—a self-saturating Hebbian paradigm. *Neural Plasticity, 8*, 188.

Mongillo, G., & Amit, D. J. (2001b). Oscillations and irregular emission in networks of linear spiking neurons. *Journal of Computational Neuroscience, 11*, 249–261.

Petersen, C. C. H., Malenka, R. C., Nicoll, R. A., & Hopfield, J. J. (1998). All-or-none potentiation at CA3-CA1 synapses. *Proc. Natl. Sci. USA, 95*, 4732–4737.

Rauch, A., La Camera, G., Lüscher, H. R., Senn, W., & Fusi, S. (2002). *Neocortical pyramidal cells respond as integrate-and-fire neurons to in vivo–like input currents*. Manuscript submitted for publication.

Rubin, J., Lee, D. D., & Sompolinsky, H. (2001). Equilibrium properties of temporally asymmetric Hebbian plasticity. *Physical Review Letters, 86*, 364–366.
Sakay, K., & Miyashita, Y. (1991). Neural organization for the long-term memory of paired associates. *Nature, 354*, 152–155.
Sjöström, P. J., Turrigiano, G. G., & Nelson, S. B. (2001). Cooperativity and frequency dependence of spike timing–dependent plasticity in visual cortical layer-5 pairs. In *Proceedings of the 31st SFN Meeting*. San Diego.
Steele, P. M., & Mauk, M. D. (1999). Inhibitory control of LTP and LTD: Stability of synapse strength. *Journal of Neurophysiology, 81*, 1559–1566.
Tsodyks, M. V., & Markram, H. (1997). The neural code between neocortical pyramidal neurons depends on neurotransmitter release probability. *Proc. Natl. Sci. USA, 94*, 719–723.
van Vreeswijk, C. A., & Sompolinsky, H. (1996). Chaos in neural networks with balanced excitatory and inhibitory activity. *Science, 274*, 1724–1726.

Received December 13, 2001; accepted August 2, 2002.